Communication

Composite Oxide Fibres Grown by Internal Crystallisation Method

Sergei Mileiko *, Andrew Kolchin, Vyacheslav Kiiko and Natalia Novokhatskaya

Institute of Solid State Physics of RAS, 2 Academician Ossypian Str., Chernogolovka Moscow Distr., 142432 Chernogolovka, Russia; an.kolchin@gmail.com (A.K.); kiiko@issp.ac.ru (V.K.); novoch@issp.ac.ru (N.N.)

* Correspondence: mileiko@issp.ac.ru; Tel.: +7-496-522-2493

Abstract: The internal crystallisation method (ICM) allows producing bundles containing hundreds and thousands of the fibres of a limited length. It is shown in the present paper that ICM can be used to produce fibres composed of a sapphire matrix and inclusions of calcium hexaaluminate. The fabrication of such composite fibres is described in the present paper. An effect of the calcium hexaaluminate inclusions in sapphire fibres is evaluated by testing model composites with brittle molybdenum matrices. The critical stress intensity factors of composite-fibre/molybdenum-matrix specimens are higher than those of specimens reinforced with sapphire fibres. The model specimens reveal non-linear stress/strain behaviour. The results of this work show the effectiveness of composite fibres as a reinforcement for brittle matrices.

Keywords: ceramic fibre; composites; mechanical testing; fracture toughness; microstructure; internal crystallisation method

1. Introduction

It is well known that a brittle-matrix/brittle-fibre composite can reveal quasi-plastic behaviour determined by the crack arrest by a "weak" fibre/matrix interface [1,2]. A usual way to organise such a kind of the interface is by coating a continuous fibre with an appropriate material. For example, in the case of oxide-fibre/oxide-matrix composites, polycrystalline fibres are often coated with calcium hexaaluminate $CaAl_{12}O_{19}$ (CA6) [3]. The values of lattice parameters of CA6 are a = 0.47597 nm, c = 2.29918 nm [4], which make the substance mica-like. "Weak" oxides like monazites [5] can also be an interphase in such composites. Actually, this approach is not limited to oxide/oxide composites: SiC_f/SiC_m composites can be non-brittle due to an interphase with similar properties [2].

The oxide/oxide composites mentioned above are based on polycrystalline oxide fibres that creep at rather low temperatures [6,7], so the use temperature of composites with such fibres is limited to a temperature of about 1200 °C [8]. Single crystalline fibres, which are much more creep-resistant, are normally obtained by technologies of low productivity rates such as Edge Feed Groeth [9], Laser Heated Pedestal Growth [10], and μ-pulling down [11]. Fibres produced by these methods are characterised by a nearly ideal microstructure, but they are too expensive to be used as reinforcement for structural composites [6]. Hence, the internal crystallisation method (ICM) to produce single crystalline fibres, which is based on the crystallisation of oxides in cylindrical channels of an auxiliary matrix, is characterised by the much higher a productivity rate than is characteristic for the traditional methods, which makes ICM-fibres suitable for structural applications. The method has been successfully used to produce a large family of single crystalline and eutectic oxide fibres [6]. The state of the art of ICM technology is described in a recent review paper [12].

The usage of ICM yields a bundle containing hundreds and thousands of the fibres. It is possible to coat a bundle of ICM-fibres with an appropriate oxide layer [13]. However, the process is a multi-step

and time-consuming one. Hence, coating the fibre at the production stage presents an attractive problem to be solved. In the present paper, ICM is used to obtain fibres composed of a strong sapphire matrix and inclusions of calcium hexaaluminate. The preliminary experiments described show a possibility of producing such fibres. An effect of the CA6 inclusions in sapphire fibres is evaluated by testing model composites with brittle molybdenum matrices.

2. Fabrication of Composite Fibres

The aim of the present work was to obtain sapphire/CA6 composite oxide fibres by using the internal crystallisation method, which is actually the crystallisation of an appropriate melt in the cylindrical continuous channels of a molybdenum matrix [6,12]. The molybdenum matrix is normally made by diffusion bonding of an assemblage of molybdenum foil and wires, so that two surfaces of the fibre are flat. After the crystallisation is completed, molybdenum can be dissolved in a mixture of acids to obtain a bundle of fibres, as presented in Figure 1. The maximum fibre length depends on the cross-sectional size of the channels in the molybdenum auxiliary matrix and can be up to 250 mm when using existing laboratory equipment. The characteristic cross-sectional size is about 0.1 mm.
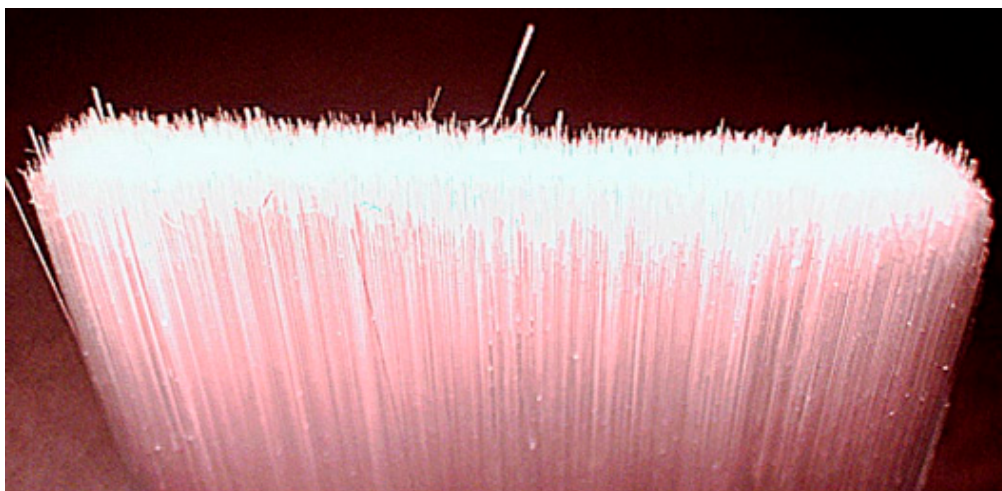

Figure 1. A bundle of sapphire fibres obtained by the method of internal crystallisation. The bundle width is 30 mm.

When dealing with a bundle of ICM-fibres as reinforcements for brittle matrix composites, it is not necessary to use a coating procedure. If we manage to crystallise fibres composed of a sapphire matrix and calcium hexaaluminate inclusions then we will have composite fibres capable of arresting cracks in the same manner as the interphase located on the periphery of a continuous fibre. Such composite fibres can be obtained by crystallising the melt of an alumina/calcia mixture.

Since the crystallisation mechanisms of such mixtures have not yet been studied, in the present experiments the mixtures containing molar fraction α of calcia between 0.021 and 0.042 were prepared. After compacting tablets with a diameter of 20 mm, the mixtures underwent pressure-less sintering at 1250 °C for 6 h. Then, a tablet was placed in a molybdenum crucible and melted in vacuum. Molybdenum carcass with cylindrical channels moved into the melt, which infiltrated the carcass. The oxide/molybdenum block then was pulled up to a cold zone of the furnace and the crystallisation of the oxides occurred. The pulling rate of the oxide/molybdenum blocks in the crystallisation process varied from zero (crystallisation took place from the top to bottom of the block as a result of a temperature gradient in the furnace) to 1000 mm/min. Specimens with pure sapphire were also prepared from the melt obtained from pieces of alumina.

Technically, pure molybdenum used in the present experiments for the carcasses recrystallises after heating up to the melting temperature of the oxide mixtures, about 2000 °C according to the Al_2O_3-CaO phase diagram [14], and becomes brittle.

Oxide-fibre/molybdenum-matrix composite specimens of two sizes were produced, namely $5 \times 5 \times 65$ mm^3 for measuring the bending strength and recording load/displacement curves (type I specimens) and $5 \times 15 \times 65$ mm^3 for measuring the critical stress intensity factor (type II specimens). Fibre volume fraction measured in eight arbitrary chosen specimens of type II was between 30 and 40%.

3. Microstructure of the Fibres

A Scanning Electron Microscope VEGA TS 5130MM (TESCAN, Brno, Czech Republic) equipped with both detecting devices for secondary (SE) and backscatter (BSE) electrons on YAG-crystals and an Energy Dispersive X-ray (EDX) spectrometer (Oxford Instruments, Oxford, UK) with semiconductor detector INCA Energy 200 were used to study the microstructures of the fibres.

At present, only preliminary information on the microstructure of the oxide composite fibres has been obtained because a study of the microstructure should be, first of all, complementary to a study of the crystallisation mechanisms of the $(1-\alpha)Al_2O_3/\alpha CaO$ melts in the channels of the molybdenum carcass. This remains to be carried out. It should be noted that in the Al_2O_3-CaO system, there are a number of the complex oxides in addition to $CaAl_{12}O_{19}$ (CA6), namely $CaAl_4O_7$, $CaAl_2O_4$, and $Ca_3Al_2O_6$ [4]. An occurrence of these oxides in the fibres is not to be excluded.

Figures 2 and 3 illustrate the typical microstructure of the fibres. Table 1 contains results of the X-ray microanalysis in some points of the fibres. Note that:

(1)   The "black" phase corresponds to alumina; "grey" phases of various degrees of darkness correspond to various calcium aluminates (CAs).
(2)   The sizes of the CAs inclusions are too small to measure Al:Ca atomic rations given precisely. Still, it is clear that all the CAs including CA6 are present in the fibres.
(3)   The configuration of the inclusion systems in the fibre seen in a longitudinal section of a composite (Figure 3a) is determined, perhaps, by special conditions of fibre crystallisation in the molybdenum carcass determined by the high thermal conductivity of molybdenum, which determines the radial temperature gradients.
(4)   A difference in the appearance of the fibre microstructures in Figure 3a, Figure 1b is mainly determined by the difference in the crystallisation rate being ~250 and <1 mm/min, respectively. Increasing the crystallisation rate yields a decrease in the characteristic size of the fibre microstructure. Obviously, the temperature gradient in the crystallisation zone affects the fibre microstructure as well. In all the present experiments, the gradient was ~1.5 °C/mm.
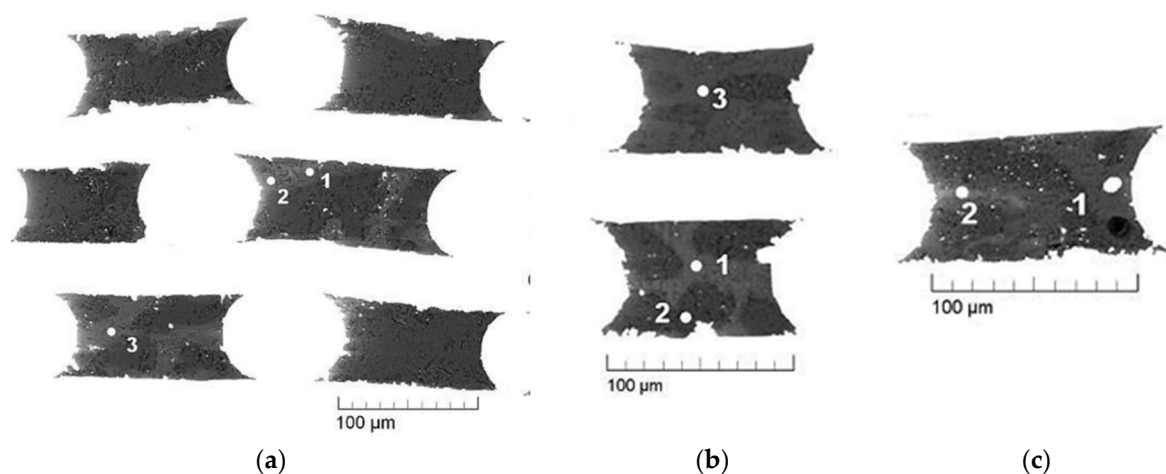

(a)   (b)   (c)

Figure 2. SEM-micrographs of fragments of a cross-section of a specimen with fibres crystallised with a crystallisation rate of ~2 mm/min; $\alpha = 0.032$. The results of the X-ray microanalysis in the points shown in the micrographs are presented in Table 1.
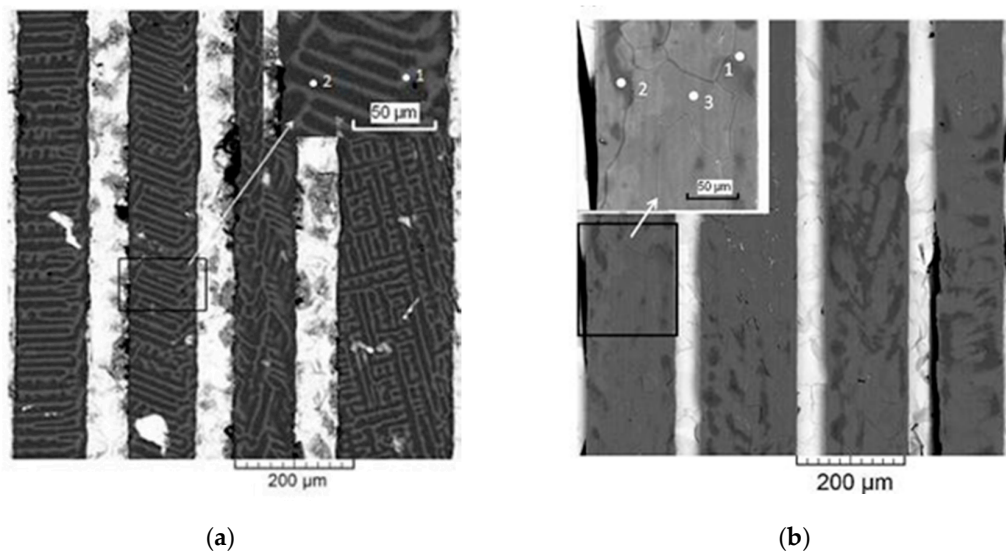
(**a**)　　　　　　　　　　　　　　　　　　　　　　(**b**)

Figure 3. SEM-micrographs longitudinal sections of specimens with fibres crystallised with a crystallisation rate of ~250 mm/min, α = 0.021 (**a**) and <1 mm/min, α = 0.032 (**b**). The results of the X-ray microanalysis in the points shown in the micrographs are presented in Table 1.

Table 1. Characteristics of the fibre microstructures and fracture toughness of oxide/molybdenum composites.

Figure	Point	α	Crystallisation Rate/mm/min	Al:Ca	Compound	$K^*/MPa \cdot m^{1/2}$
Figure 2a	**1**	**0.032**	**2**	**11**	$\mathbf{CaAl_{12}O_{19}}$	**22.5**
	2	0.032	2	11	$CaAl_{12}O_{19}$	
	3	0.032	2	9.4	$CaAl_{12}O_{19}$	
Figure 2b	1	0.032	2	4.3	$CaAl_4O_7$	
	2	0.032	2	>100	Al_2O_3	
	3	0.032	2	11	$CaAl_{12}O_{19}$	
Figure 2c	1	0.032	2	10	$CaAl_{12}O_{19}$	
	2	0.032	2	2	$CaAl_2O_4$	
Figure 3a	1	0.021	250	4	$CaAl_4O_7$	22.7
	2	0.021	250	>100	Al_2O_3	
Figure 3b	1	0.032	<1	10	$CaAl_{12}O_{19}$	16.3
	2	0.032	<1	14	$CaAl_{12}O_{19}$	
	3	0.032	<1	4	$CaAl_4O_7$	

The X-ray diffraction pattern taken from a cross-section of a specimen with α = 0.032 obtained at a pulling rate of 50 mm/min shows the existence of three oxides, Al_2O_3, $CaAl_{12}O_{19}$ (CA6), and $Ca_3Al_2O_6$. This is in accordance with the observations just described.

These observations call for the further study of crystallisation mechanisms to relate the results with the fibre microstructure and the effectiveness of CA6 inclusions as a crack arresting means. Obviously, it will be necessary to find ways to control the crystallographic orientation of the inclusions and their optimal volume fractions, etc.

4. Mechanical Properties of Oxide/Molybdenum Composites

All mechanical tests were performed on a universal testing machine produced by Russian company NIKIMP.

The most important testing of the model oxide/molybdenum composites is measuring the critical stress intensity factor K^*. Most of the specimens of type II used in these experiments had a radius

of the notch tip made by a diamond tool equal to 0.15 mm, although some of the specimens had a radius of 0.5 mm. Preliminary experiments did not reveal a noticeable difference in the results of testing specimens with different notch radii. Length *c* of the notch was equal to approximately half the height *h* of the specimen. The notch was oriented with respect to the fibres, as shown in Figure 4. The specimens were tested in three-points bending with the displacement rate of the cross-head being 10 mm/min. Typical load/displacement curves are presented in Figure 5.

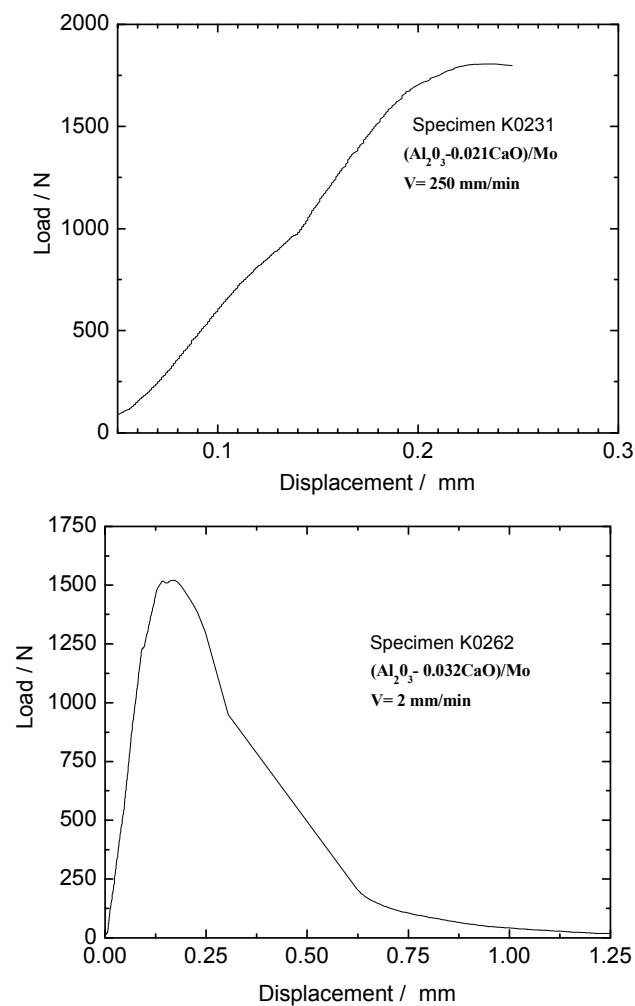**Figure 4.** Schematic of a specimen with the notch.

Figure 5. Typical load/displacement curves for composites with composite fibres. The fibre microstructures of specimens K0231 and K0262 are presented in Figures 2 and 3a, respectively.

Measuring the critical stress intensity factor was not aimed at obtaining the values to be used in calculating the ultimate load of a structural element. The aim was just to evaluate an effect of the highly anisotropic oxide inclusions in sapphire fibres on the fracture toughness of a composite with a brittle matrix (recrystallised molybdenum). Therefore, it was not necessary to follow all the requirements of the corresponding standards developed to characterize metals and ceramics. The standards recommend the specimen sizes and the rules for using the value of a load in formulae giving the values of *K**; a requirement to sharpen the notch tip by fatigue loading is also written in the standards. Still, the calculation of the values of *K** was performed by taking maximum load *Q* on the load/displacement curve by using the formula recommended by ASTM E 399-90 Standard:

$$K^* = \frac{3QLc^{1/2}}{2h^2 w} Y\left(\frac{c}{h}\right)$$

where

$$Y = \left[1.96 - 2.75\frac{c}{h} + 13.66\left(\frac{c}{h}\right)^2 - 23.98\left(\frac{c}{h}\right)^3 + 25.22\left(\frac{c}{h}\right)^4\right].$$

Here, *L* is distance between the supports, *w* is width of the specimen. The sizes in the present experiments were $L \approx 60$ mm, $h \approx 15$ mm, $w \approx 5$ mm, $c \approx (0.45 - 0.55)h$.

The dependence of the apparent critical stress intensity factor of molybdenum matrix composites with fibres crystallized from the melts with various values of α is presented in Figure 6. It should be noted that the value of *K** for the molybdenum carcass without any fibres but heated up to a temperature causing its infiltration into the oxide melts is less than 9 MPa·m$^{1/2}$; the same parameter for sapphire-fibre/molybdenum matrix composites is 15.7 ± 3.6 MPa·m$^{1/2}$. Some important observations can now be formulated.

First, at least two fabrication parameters of the composites with composite fibres affect the material properties, those being (i) the composition of the raw mixture of oxides and (ii) the crystallisation rate. The largest values of critical stress intensity factor *K** were obtained for the oxide mixture with a molar concentration of calcium between 0.021 and 0.032 and for a crystallisation rate V_c between 2 and 10 mm/min.
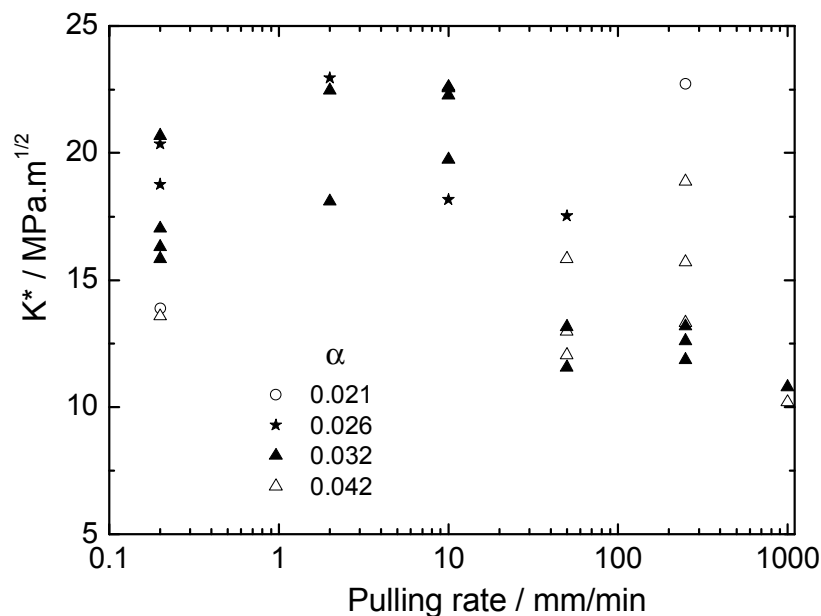

Figure 6. Critical stress intensity factor of oxide-fibre/molybdenum-matrix composites versus pulling rate.

Secondly, the value of K^* for the composite specimens obtained within the intervals of α and V_c mentioned is 21.5 ± 1.8 MPa·m$^{1/2}$, which is really higher than that for sapphire-fibre/molybdenum matrix composites.

Thirdly, the fracture zone in front of the notch in the composite reinforced with composite fibres, Figure 7, contains chains of the local delaminations at the "weak" inclusions. Such a size of the fracture zone is typical for composites and this makes methods of linear fracture mechanics not applicable to the estimation of the ultimate load of a structural element containing defects. The values of K^* of the composites can be used only for the comparison of various composite microstructures with regard to their notch sensitivity. The ratio σ_N^*/σ_o^* of the values of strength σ_N^* of a specimen with notch to that of the un-notched specimen, σ_o^*, serves the same purpose. Note that there exists a correlation between K^* and σ_N^*/σ_o^* [15]. Figure 8 illustrates this correlation for the composites, for which $K^* = 21.5 \pm 1.8$ MPa·m$^{1/2}$. The procedure to evaluate ratio σ_N^*/σ_o^* is described in detailed in Reference [15]. Note that for the composites under consideration, $\sigma_N^*/\sigma_o^* = 0.68 \pm 0.10$.

In the second series of the experiments, the load/displacement curves in the three-point bending of type I specimens without the notch were recorded. The applied load was normal to the flat surfaces of the fibres. A typical curve for a specimen with composite fibres is presented in Figure 9. Unlike the curves for specimens with pure sapphire fibre, which are linear, this curve is obviously non-linear. The dependence of the bending strength of oxide/molybdenum specimens with composite fibres crystallised from the $(1-\alpha)Al_2O_3/\alpha CaO$ raw mixtures, $\alpha = 0.021$ and 0.042, and corresponding fibres on pulling rate in the fabrication process of the composites is presented in Figure 10. The composite strength was obtained by testing specimens of type I, and the fibre strength was evaluated by using the experimental data and assuming a molybdenum carcass strength equal to 450 MPa [16] and a fibre volume fraction equal to 0.35. A correlation between these dependencies and the dependencies of the critical stress intensity factor on the pulling rate, presented in Figure 6, can be traced, but more experiments should be performed to justify the possible correlation.
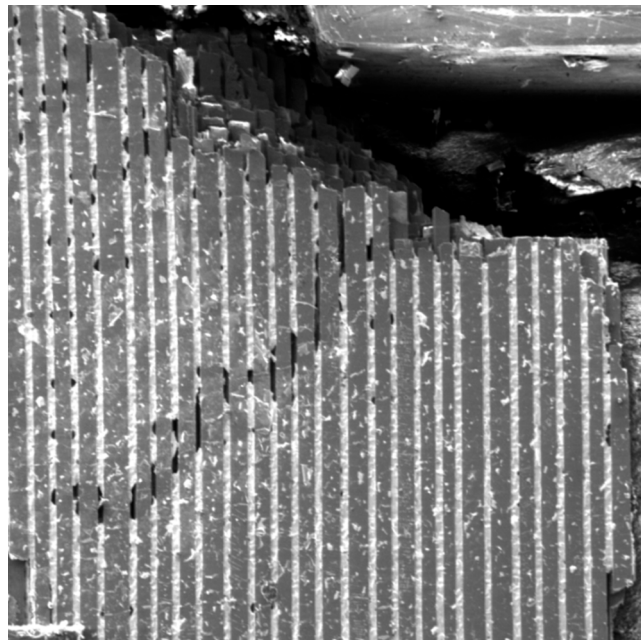

Figure 7. Fracture zone in front of the notch seen as a plane line at the right side. The same specimen as shown in Figure 3a; see also Table 1.
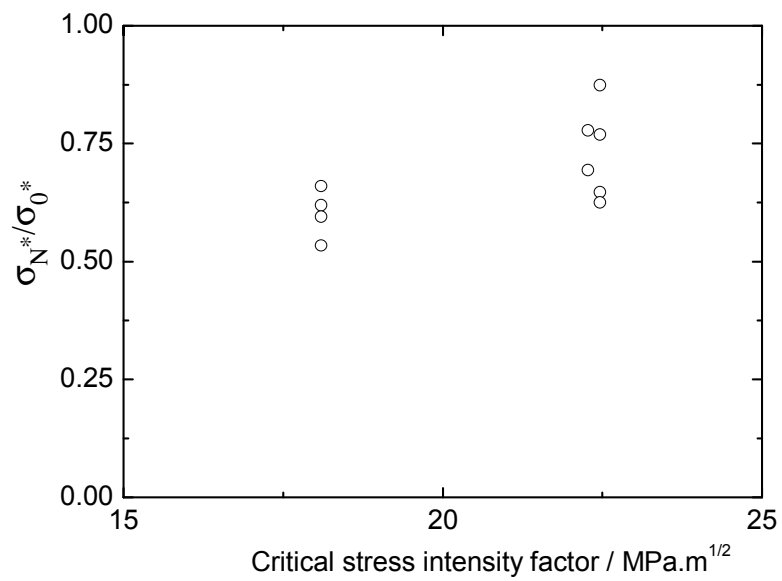
Figure 8. Correlation between the critical stress intensity factor and notch sensitivity for composite-fibre/molybdenum-matrix composites.
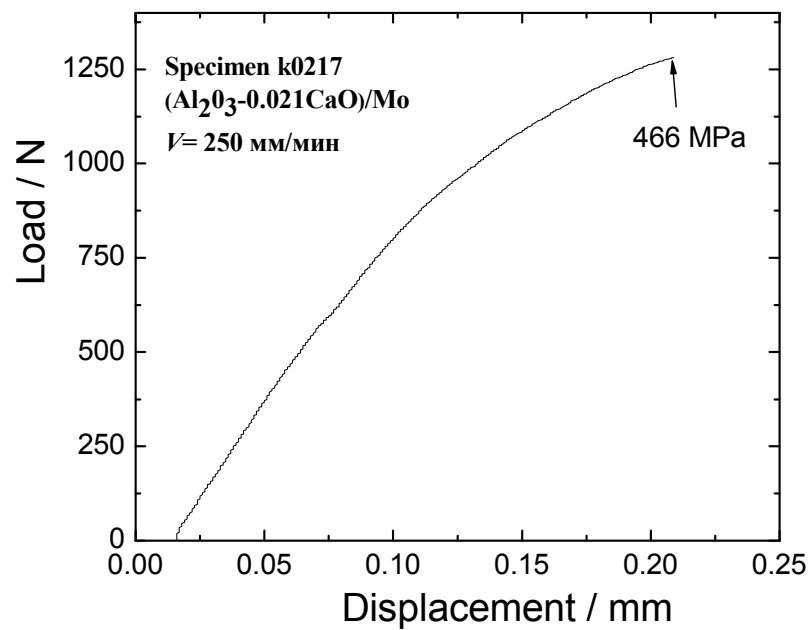

Figure 9. The load/displacement curve obtained in the three-point bending of a composite specimen.
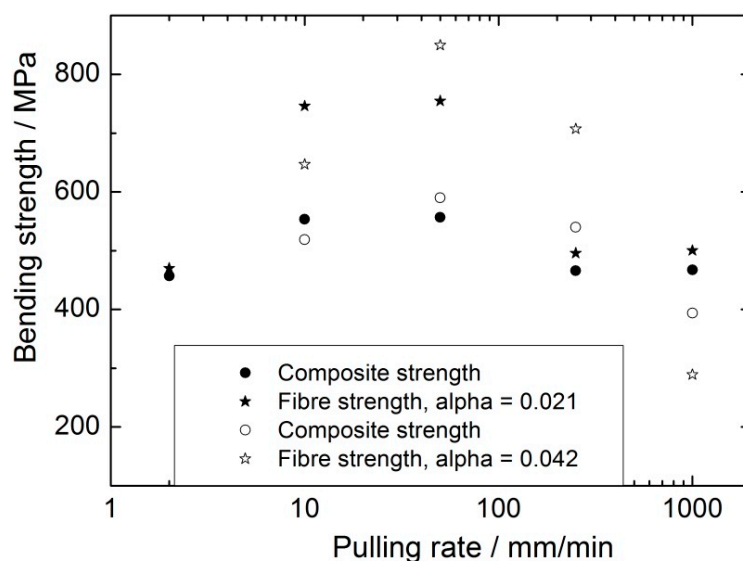
Figure 10. Strength of specimens of type I and reinforcing fibres versus crystallisation rate. Solid and open points represent the composites containing fibres obtained from the raw oxide mixtures with α = 0.021 and 0.042, respectively.

5. Conclusions

1. A possibility of obtaining oxide fibres composed of sapphire and calcium aluminate inclusions by using the internal crystallisation method is shown.
2. Measurements of fracture toughness and observation of the microstructure of the fracture zone in front of the notch tip of the model composites with brittle molybdenum matrices and the oxide fibres containing CA6-inclusions show that such inclusions can arrest crack propagation.
3. At present, the crystallisation mechanisms of oxide fibres with CA6-inclusions is not completely clear. Optimisation of the microstructures and the crystallisation process is necessary to make oxide composite fibres for important reinforcements for brittle matrices to launch a new type of brittle-fibre/brittle-matrix composite with a quasi-plastic behaviour.

Author Contributions: S.M. conceived and designed the experiments, analyzed the data, wrote the paper; A.K. conceived the experiments; V.M. conducted the mechanical tests; N.N. observed the microstructures.

Conflicts of Interest: The authors declare no conflict of interest. The founding sponsors had no role in the design of the study; in the collection, analyses, or interpretation of data; in the writing of the manuscript, and in the decision to publish the results.

References

1. Aveston, J.; Cooper, G.A.; Kelly, A. Single and multiply fracture, the properties of fibre composites. In Proceedings of the Conference the Properties of Fibre Composites, National Physical Laboratory, Teddington, UK, 4 November 1971; IPC Science and Technology Press Ltd.: Teddington, UK, 1971; pp. 15–26.
2. Naslain, R.; Dugne, O.; Guette, A.; Sevely, J.; Robin-Brosse, C.; Rocher, J.P.; Cotteret, J. Boron nitride interphase in ceramic matrix composites. *J. Am. Ceram. Soc.* **1991**, *74*, 2482–2488. [CrossRef]
3. Cinibulk, M.K. Hexaluminates as a cleavable fiber–matrix interphase: Synthesis, texture development, and phase compatibility. *J. Eur. Ceram. Soc.* **2000**, *20*, 569–582. [CrossRef]
4. Institute of Experimental Mineralogy, Chernogolovka, Russia. Available online: http://database.iem.ac.ru/mincryst/s_carta.php?HIBONITE (accessed on 9 January 2016).

5. Kuo, D.H.; Kriven, W.M.; Mackin, T.J. Control of interfacial properties through fiber coatings: Monazite coatings in oxide-oxide composites. *J. Am. Ceram. Soc.* **1997**, *80*, 2987–2995. [CrossRef]

6. Mileiko, S.T. Single crystalline oxide fibres for heat-resistant composites. *Compos. Sci. Technol.* **2005**, *65*, 2500–2513. [CrossRef]

7. Wilson, D.M.; Visser, L.R. High performance oxide fibers for metal and ceramic composites. *Compos. Part A* **2001**, *32*, 1143–1153. [CrossRef]

8. Keller, K.A.; Jefferson, G.; Kerans, R.J. Oxide–oxide composites. In *Ceramic Matrix Composites: Materials, Modeling and Technology*; Bansal, N.P., Lamon, J., Eds.; Wiley: Hoboken, NJ, USA, 2014.

9. LaBelle, H.E., Jr.; Mlavsky, A.I. Growth of sapphire filaments from the melt. *Nature* **1967**, *216*, 574–575. [CrossRef]

10. Burrus, C.A.; Coldren, L.A. Growth of single-crystal sapphire-clad ruby fibers. *Appl. Phys. Lett.* **1977**, *31*, 383–384. [CrossRef]

11. Yoon, D.H.; Fukuda, T. Characterization of LiNbO$_3$ micro single crystals grown by the micro-pulling-down method. *J. Cryst. Growth* **1994**, *144*, 201–206. [CrossRef]

12. Mileiko, S.T. Internal crystallisation method to produce oxide fibres and heat resistant composites. In *Recrystallization in Materials Processing*; Glebovsky, V., Ed.; InTech: Rijeka, Croatia, 2015; pp. 125–168. Available online: http://www.intechopen.com/books/recrystallization-in-materials-processing/internal-crystallisation-method-to-produce-oxide-fibres-and-heat-resistant-composites (accessed on 15 August 2017).

13. Popova, N.A.; Tolstun, A.N. A monazite imterphase in oxide/oxide composites with ICM-fibrers. *Sci. Ind.* **2007**, *2*, 58–61. (In Russian)

14. Phase Equilibria Diagrams, ACerS–NIST. 2003. Version 3. CD-ROM Database. Available online: http://ceramics.org/publications-and-resources/phase-equilibria-diagrams (accessed on 20 August 2017).

15. Mileiko, S.T. Fracture-toughness/notch-sensitivity correlation for metal- and ceramic-based fibrous composites. *Compos. Part B* **2017**, *116*, 1–6. [CrossRef]

16. Mileiko, S.T.; Kazmin, V.I. Structure and mechanical properties of oxide fibre reinforced metal matrix composites produced by the internal crystallisation method. *Compos. Sci. Technol.* **1992**, *45*, 209–220. [CrossRef]